Nonlinear Dyn (2016) 84:1877–1882
DOI 10.1007/s11071-016-2612-9

ORIGINAL PAPER

Light bullet supported by parity-time symmetric potential with power-law nonlinearity

Si-Liu Xu · Nikola Petrović · Milivoj R. Belić · Zheng-Long Hu

Received: 17 November 2015 / Accepted: 9 January 2016 / Published online: 27 January 2016
© Springer Science+Business Media Dordrecht 2016

Abstract Using a similarity transformation, we find the light bullet solution of $(3+1)$-dimensional nonlinear Schrödinger equation with parity-time (PT) symmetric potential. The diffraction/dispersion and nonlinearity coefficients are chosen as longitudinally inhomogeneous functions. We demonstrate how intensity, width, phase, and chirp of the solution are modulated by the variation in diffraction/dispersion and by the choice of PT-potential. Dynamic characteristics of light bullets in media described by exponentially decreasing diffraction/dispersion and periodically modulated systems are illustrated.

Keywords Light bullet · Parity-time symmetry · Nonlinear Schrödinger equation

S.-L. Xu (✉) · Z.-L. Hu
The School of Electronic and Information Engineering, HuBei University of Science and Technology, Xianning 437100, China
e-mail: xusiliu1968@163.com

N. Petrović · M. R. Belić
Texas A&M University at Qatar, P.O. Box 23874, Doha, Qatar

M. R. Belić
Institute of Physics, University of Belgrade, P.O. Box 68, Belgrade 11001, Serbia

1 Introduction

Solitons in spatially inhomogeneous media have attracted great attention in the past decade, owing to numerous applications in many areas of physics such as photonic devices, nonlinear plasmas, fluid dynamics, and Bose–Einstein condensation (BEC) [1–5]. Recently, the propagation of localized optical beams in complex nonlinear media featuring parity-time (PT) symmetry has become a subject of intense study [6–10].

The PT-symmetry became important in quantum mechanics when Bender and Boettcher in 1998 showed that Hamiltonians with such symmetry can have an entirely real spectrum, although the Hamiltonians are non-Hermitian [11]. Complex PT-symmetric potentials require that the real part of the potential must be an even function of position, whereas the imaginary part should be odd. Another important property of PT-symmetric system is the existence of a sudden phase transition known as the spontaneous PT-symmetry breaking, above which the spectrum ceases to be real.

Nowadays, the properties of solitons in the form of ultrashort and strong laser pulses are quite well known [12–14]. Furthermore, in the long-distance communications and all-optical ultrafast switching devices, many spatiotemporal localized structures such as optical solitons [15], similaritons [16], and light bullets (LBs) [17] have been displayed in nonlinear optics. However, spatiotemporal localized structures in PT-symmetric potentials have not been discussed much. Especially, the 3D solitons in PT-symmetric potentials

with power-law nonlinearities are hardly reported [18]. This study is undertaken in this paper.

The plan of this paper is as follows. In Sect. 2, we briefly introduce the general model and obtain a distinct type of soliton solution. In Sect. 3, the dynamic characteristics of light bullets (LBs), such as their intensity, width, phase, and chirp in specially designed media, are studied. Numerical simulations and comparison with the analytical results are performed in the same section. In Sect. 4, the conclusion to the paper is outlined briefly.

2 The model and the soliton solutions

We present here analytical LB solutions to the general (3 + 1)-dimensional nonlinear Schrödinger equation (NLSE)

$$i\partial_z u + \frac{\beta(z)}{2}(\nabla_\perp u + \partial_t^2 u) + \chi(z)|u|^{2m}u + [v(z,r) + iw(z,r)]u = 0 \tag{1}$$

with the power-law nonlinearity and a PT-symmetric potential. Here, $\nabla_\perp = \partial^2/\partial x^2 + \partial^2/\partial y^2$ is the transverse Laplacian, $r \equiv (x, y, t)$ is the position vector, and $u(z, r)$ is the complex envelope of the electric field, normalized with $(k_0 w_0)^{-1}(n_2/n_0)^{-1/2}$. The longitudinal z, transverse x, y coordinates, and the comoving time t are, respectively, scaled by the diffraction length $L_D \equiv k_0 w_0^2$ (with the wave number $k_0 \equiv 2\pi n_0/\lambda$), the typical input spatial width w_0, and the temporal pulse width. Functions $\beta(z)$ and $\chi(z)$ denote the diffraction/dispersion (DD) and the nonlinearity coefficients, respectively. An even function $v(z, r) \equiv k_0^2 w_0^2 n_R(z, r)$ and an odd function $w(z, r) \equiv k_0^2 w_0^2 n_I(z, r)$, to be specified subsequently, are the real and imaginary components of the complex PT-symmetric potential, corresponding to the index-guiding and the gain or loss distribution of the optical potential.

To obtain exact analytical solutions of Eq. (1), we introduce a self-similar transformation of the solution sought [16,17]:

$$u(z,r) = A(z)U[X(z,x), Y(z,y), T(z,t), Z(z)]e^{i\varphi(z,r)}. \tag{2}$$

where $A(z)$ is the amplitude; $X = X(x, z)$, $Y = Y(z, y)$, and $T = T(z, t)$ are the formal self-similar variables; $Z = Z(z)$ is the effective propagation distance; and $\varphi(z, r)$ is the phase of the wave, all assumed to be real functions. Substituting Eq. (2) into Eq. (1), one obtains the following standard NLSE with constant nonlinearity coefficient χ_0:

$$i\frac{\partial U}{\partial Z} + \frac{1}{2}\left[\frac{\partial^2 U}{\partial X^2} + \frac{\partial^2 U}{\partial Y^2} + \frac{\partial^2 U}{\partial T^2}\right] + \chi_0|U|^{2m}U + [V(X,Y,T) + iW(X,Y,T)]U = 0, \tag{3}$$

with the requirements that:

$$\chi_0 = \frac{A_0^{2m}\chi(z)}{\beta(z)[1 - s_0\int\beta(z)\mathrm{d}z]^{3m-2}}, \tag{4a}$$

$$V(X,Y,T) = \frac{[1 - s_0\int\beta(z)\mathrm{d}z]^2}{\beta(z)}v(z,r), \tag{4b}$$

$$W(X,Y,T) = \frac{[1 - s_0\int\beta(z)\mathrm{d}z]^2}{\beta(z)}w(z,r), \tag{4c}$$

where A_0 and s_0 are arbitrary real constants. The requirement that the new nonlinearity coefficient χ_0 is constant enforces a relation between the nonlinearity and the DD coefficient, expressed by Eq. (4a). Thus, in order for the method of solution to be valid and the prescribed LB solutions obtained, an integrability condition on the method must be imposed, in the form of Eq. (4a). After some algebra, the simplest particular solutions are obtained:

$$A = A_0[1 - s_0\int\beta(z)\mathrm{d}z]^{3/2},$$

$$X(z,x) = \frac{x}{1 - s_0\int\beta(z)\mathrm{d}z}, \tag{5a}$$

$$Y(z,y) = \frac{y}{1 - s_0\int\beta(z)\mathrm{d}z},$$

$$T(z,t) = \frac{t}{1 - s_0\int\beta(z)\mathrm{d}z}, \tag{5b}$$

$$Z(z) = \frac{\int\beta(z)\mathrm{d}z}{1 - s_0\int\beta(z)\mathrm{d}z},$$

$$\varphi(z,r) = -\frac{s_0(x^2 + y^2 + z^2)}{2[1 - s_0\int\beta(z)\mathrm{d}z]}. \tag{5c}$$

Solutions of Eq. (3) can be considered as seeds which generate various solutions of Eq. (1) via relations (4) under conditions (5). Therefore, if we substitute solutions of Eq. (3) into transformation (2), nonautonomous solitons of Eq. (1) can be obtained.

Here, we investigate the localized modes supported by a 3D PT-symmetric complex potential $V_{PT}(X, Y, T)$ whose real and imaginary parts are given by:

$$V = V_0(X^2+Y^2+T^2) - V_1 e^{-2a^2(X^2+Y^2+T^2)} + V_2(e^{-2a^2X^2} + e^{-2a^2Y^2} + e^{-2a^2T^2}) \quad (6a)$$

and:

$$W = W_0(Xe^{-a^2X^2} + Ye^{-a^2Y^2} + Te^{-a^2T^2}), \quad (6b)$$

which satisfy the properties of PT-symmetry: $V(X, Y, T) = V(-X, -Y, -T)$ and $W(X, Y, T) = -W(-X, -Y, -T)$.

We seek a solution of 3D NLSE (3) in the form:

$$U(Z, X, Y, T) = \psi(X, Y, T)e^{i\delta z+\theta(X,Y,T)}. \quad (7)$$

Here, the real-valued functions of phase $\theta(X, Y, T)$ and amplitude $\psi(X, Y, T)$ satisfy the following differential equations:

$$\nabla^2\psi - |\nabla\theta|^2\psi + V(r)\psi + \chi_0\psi^{2m+1} = \delta\psi, \quad (8a)$$

$$\psi\nabla^2\theta + 2\nabla\theta\cdot\nabla\psi + W(r)\psi = 0. \quad (8b)$$

For potential (6), the above equations possess closed-form localized solutions that satisfy $\psi(X, Y, T) \to 0$ when $(X, Y, T) \to \pm\infty$. Thus, for the amplitude, we obtain:

$$\psi(X, Y, T) = \left|\frac{V_1}{\chi_0}\right|^{\frac{1}{2m}} e^{-\frac{a^2(X^2+Y^2+T^2)}{m}} \quad (9a)$$

while the phase $\theta(X, Y, T)$ is given by:

$$\theta(X, Y, T) = \frac{mW_0\sqrt{\pi}}{4a^3(m+2)}[\mathrm{Erf}(aX) + \mathrm{Erf}(aY) + \mathrm{Erf}(aT)]|, \quad (9b)$$

where $\mathrm{Erf}(X, Y, Z)$ is the error function, $V_0 = -4a^4/m^2$, $V_2 = -m^2W_0^2/4a^2(m+2)^2$, and $\delta = -4a^4/m$.

From expression (2), the components of the complex PT-potential are given as:

$$v = \frac{\beta(z)}{[1 - s_0\int\beta(z)]^2}[V_0(X^2+Y^2+T^2) - V_1e^{-2a^2(X^2+Y^2+T^2)} + V_2(e^{-2a^2X^2} + e^{-2a^2Y^2} + e^{-2a^2T^2})] \quad (10a)$$

and

$$w = \frac{W_0\beta(z)}{[1 - s_0\int\beta(z)\mathrm{d}z]^2}(Xe^{-a^2X^2} + Ye^{-a^2Y^2} + Te^{-a^2T^2}). \quad (10b)$$

The soliton solution of Eq. (1) is thus:

$$u(z, r) = \frac{A_0}{[1 - s_0\int\beta(z)\mathrm{d}z]^{3/2}}\left|\frac{V_1}{\chi_0}\right|^{\frac{1}{2m}} e^{-\frac{a^2(X^2+Y^2+T^2)}{m}+i\theta(X,Y,T)+i\varphi(z,r)+i\delta z}, \quad (11)$$

where X, Y, T, and $\varphi(t, x, y, z)$ satisfy Eqs. (5a)–(5c), respectively. Here, the phase is made up of the phase $\theta(X, Y, T)$ in solution (9b) and of the chirped phase $\varphi(z, r)$, expressed by Eq. (5c).

3 The characteristic distributions of solitons

To illustrate the characteristics of the analytic solution (11), we present the corresponding system management schemes in a DD medium (DDM) with decreasing $\beta(z) = \beta_0\exp(-\omega z)$ [19] and in the periodically modulated medium (PMM), $\beta(z) = \beta_0\cos(z)$ [20], the choice of which leads to the controlled development of nonautonomous waves.

From Eqs. (10a) and (10b), one finds that the complex PT-symmetric potential satisfies $v(x, y, t) = v(-x, -y, -t)$ and $w(x, y, t) = -w(-x, -y, -t)$. Thus, the index-guiding and the gain or loss distributions are even and odd functions with regard to x, y, and t. For the complex PT-symmetric potential, the even and odd properties of v and w are depicted in Fig. 1a, c and b, d, respectively.

Figure 2 presents the isosurface plots and the intensity distributions of LBs in the x–y plane for DDM, at different longitudinal distances. One can see that the LB exhibits a spherical distribution. Moreover, it is found that the LB profiles are self-similar and that the radii and the intensities of the pulse become slowly bigger as the propagation distance increases.

Figures 3a–c show the real part, the imaginary part, and the phase of the field distribution of the LB in the x–y plane, with $m = 1$. One sees that the real part

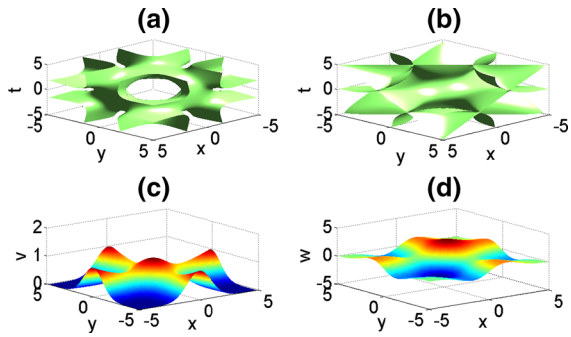

Fig. 1 Even function v and odd function w of the PT-symmetric potential, with **a**, **b** isosurface plots and **c**, **d** distributions in the x–y plane, at $z = 120, t = 1$. The remaining parameters are $\beta_0 = 0.2$, $W_0 = 0.1$, $V_1 = 2$, $\omega = 0.15$, and $s_0 = 0.4$

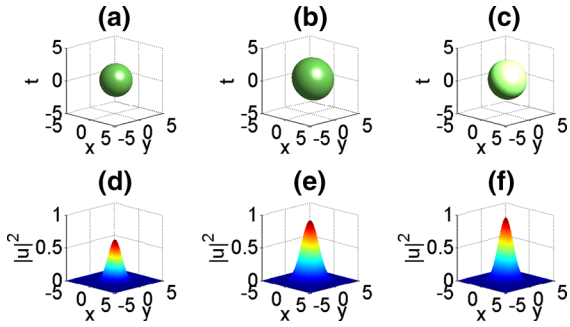

Fig. 2 Isosurface plots and intensity distributions of LBs in the x–y plane, for DDM, at different propagation distances: **a**, **d** $z = 10$, **b**, **e** $z = 100$, and **c**, **f** $z = 160$. The potential used is depicted in Fig. 1

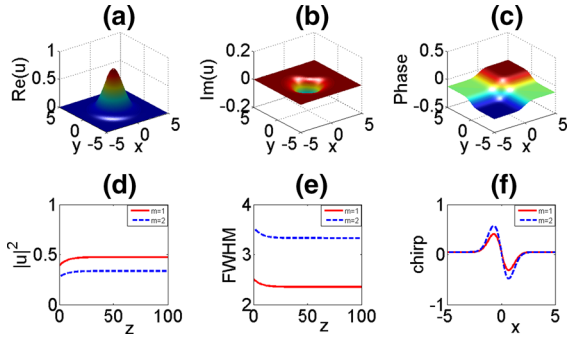

Fig. 3 **a**–**c** Real part, the imaginary part, and the phase of the field distribution of LBs in the x–y plane, with $m = 1$. **d**–**f** Intensity, half width, and the chirp of LBs, for two different values of m. Other parameters are as in Fig. 2

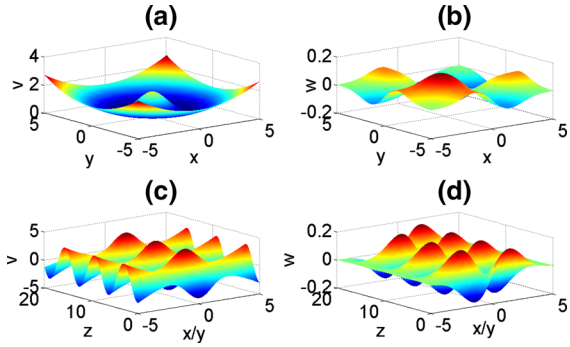

Fig. 4 **a**, **c** Even function v and **b**, **d** odd function w of the PT-symmetric potential in the PMM at **a**, **b** $z = 120$, $t = 1$ and **c**, **d** $t = 1$. The setup and other parameters are the same as in Fig. 1

of the field distribution is positive, while the imaginary part is negative and has a far lower magnitude than the real part. In Fig. 3c, an abrupt phase change is seen. The phase of the LB, as expressed in Eq. (11),

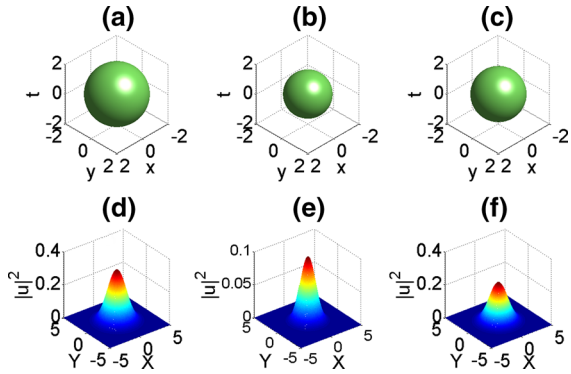

Fig. 5 Isosurface plots and the intensity distribution of LBs in x–y plane for PMM at different program distances **a**, **d** $z = 10$, **b**, **e** $z = 100$, and **c**, **f** $z = 160$. The PT-potential used is depicted in Fig. 4

is a result of the superposition of the original form, the abrupt phase change $\theta(z, r) + \delta z$ in solution (9b), and the parabolic shape $\varphi(z, r)$ in Eq. (5). Thus, the phase shows an abrupt gradient change on the parabolic background, which can be clearly seen from the top of the parabolic shape in Fig. 3c. In Fig. 3d–f, the intensity, half width, and the chirp of the LB with different m are displayed. We see that the intensity of the LB increases slightly until about $z = 15$ and afterward there is little change. On the other hand, the width decreases at first and then remains constant along the propagation distance. From Fig. 3f, it is apparent that the chirp of the LB displays an odd-symmetric property about the origin and at ± 0.75 achieves a maximum and a minimum value, respectively. Moreover, the larger the m, the smaller the intensity. However, in the case of width, the opposite holds.

Figure 4 exhibits a periodic structure of the complex PT-potential along the propagation distance z in PMM. Similar to Fig. 1, the even and odd properties of v and w are displayed in Fig. 4a, c and b, d. Along the propagation distance, the characteristics of the periodic oscillation change as shown in Fig. 4c, d.

Figure 5 presents the isosurface plot and the intensity distribution of LB in the x–y plane for PMM, at different propagation distances. Similar to Fig. 2, a spherical distribution is seen. It is shown that the LB exhibits a periodic propagation along the distance z. This property can be verified from Fig. 6d. Figures 6a–c describe the real part, the imaginary part, and the phase of the field distribution of the LB in the x–y plane, with $m = 1$. Similar to the previous case, one can see that the real

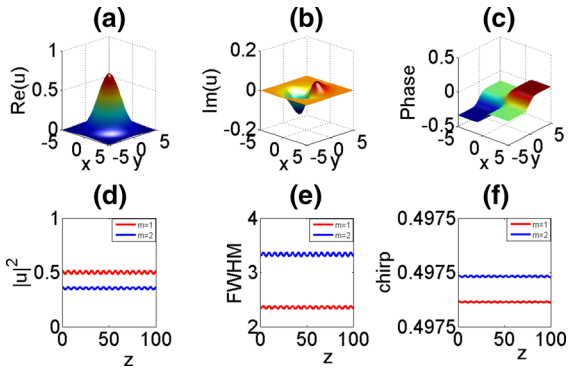

Fig. 6 **a–c** Real and imaginary parts, and the phase of field distributions of LBs in x–y plane, with $m = 1$. **d–f** Intensity, half width, and the chirp of LBs with two different values of m. The parameters are the same as in Fig. 2

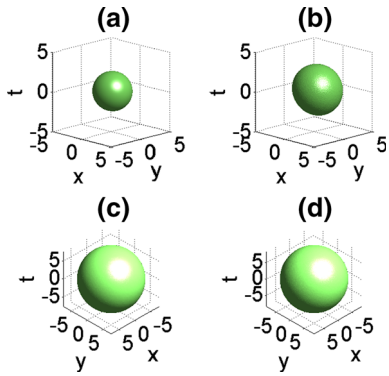

Fig. 7 Numerical simulation of LBs for DDM (**a**, **b**) and PMM (**c**, **d**) at different distances **a**, **c** $z = 100$, and **b**, **d** $z = 160$. A 5 % white noise is added to the initial field. The parameters are the same as in the analytical plots

part of the field distribution is even and that the imaginary is close to being odd and is far less in magnitude than the real part. In the same way, the abrupt phase transition is shown in Fig. 6c. When the DD parameter $\beta(z)$ is a cosine function, the periodic structure of the soliton intensity, width, and the chirp is clearly seen along the propagation direction in Fig. 5d, e. Similarly to Fig. 3, it can be seen that with an increase in m, the width and the chirp increase, while the intensity decreases.

Figure 7 shows the direct numerical integration of Eq. (1) for DDM (Fig. 7a, b) and PMM (Fig. 7a, b) at different propagation distances. We use a 3D split-step FFT beam propagation technique and consider an initial field whose form is given by Eq. (11) at $z = 0$. It is seen that the numerical calculations indicate no collapse, and stable propagation over tens of diffraction lengths is observed, except for some small oscillations. Moreover, the LB is more stable in the PMM than in the DDM. Thus, based on these results, there is strong indication that the dispersion/diffraction management of the type considered can prolong the life of LBs significantly.

4 Conclusion

In summary, we discovered LBs supported by a parity-time symmetric potential with a power-law nonlinearity. We established ways in which intensity, width, phase, and the chirp of these LBs can be modified by the variation in the diffraction/dispersion and the nonlinearity coefficients. Our results indicate that the behavior of 3D LBs in PT-lattice is considerably different from the behavior of the dissipative and the ground state solitons in the 3D case.

Acknowledgments This work is supported in China by the Natural Science Foundation of Hubei Province in China (Grant No. 2013CFB38), the Project in Hubei Province Department of Education, under Grant Q20142805, in China. Work in Qatar is supported by the NPRP 6-021-1-005 project with the Qatar National Research Fund, and additionally in China by the Natural Science Foundation of Guangdong Province, under Grant No. 1015283001000000. The work in Serbia is supported by the Serbian Ministry of Education and Science under project OI 171006. MRB acknowledges support by the Al Sraiya Holding Group.

References

1. Christodoulides, D.N., Lederer, F., Silberberg, Y.: Discretizing light behaviour in linear and nonlinear waveguide lattices. Nature **424**, 817–823 (2003)
2. Lederer, F., Stegeman, G.I., Christodoulides, D.N., Assanto, G., Segev, M., Silberberg, Y.: Discrete solitons in optics. Phys. Rep. **463**, 1–126 (2008)
3. Zhu, H.P.: Nonlinear tunneling for controllable rogue waves in two dimensional graded-index waveguides. Nonlinear Dyn. **72**, 873–882 (2013)
4. Batchelor, G.K.: An Introduction to Fluid Dynamics. Cambridge University Press, Cambridge (2000)
5. Khaykovich, L., Schreck, F., Ferrari, G., Bourdel, T., Cubizolles, J., Carr, L.D., Castin, Y., Salomon, C.: Formation of a matter-wave bright soliton. Science **296**, 1290–1293 (2002)
6. Abdullaev, FKh, Kartashov, Y.V., Konotop, V.V., Zezyulin, D.A.: Solitons in PT-symmetric nonlinear lattice, solitons in PT-symmetric nonlinear lattices. Phys. Rev. A **83**, 041805(R) (2011)

7. Alexeeva, N.V., Barashenkov, I.V., Sukhorukov, A.A., Kivshar, Y.S.: Optical solitons in PT-symmetric nonlinear couplers with gain and loss. Phys. Rev. A **85**, 063837 (2012)
8. Mayteevarunyoo, T., Malomed, B.A., Reoksabutr, A.: Solvable model for solitons pinned to a parity-time-symmetric dipole. Phys. Rev. E **88**, 022919 (2013)
9. Midya, B., Roychoudhury, R.: Nonlinear localized modes in PT-symmetric Rosen–Morse potential wells. Phys. Rev. A **87**, 045803 (2013)
10. Midya, B., Roychoudhury, R.: Nonlinear localized modes in PT-symmetric optical media with competing gain and loss. Ann. Phys. **341**, 12 (2014)
11. Bender, C.M., Boettcher, S.: Real spectra in non-hermitian Hamiltonians having PT-symmetry. Phys. Rev. Lett. **80**, 5243–5246 (1998)
12. Belyaeva, T.L., Serkin, V.N., Agüero, M.A., Hernandez-Tenorio, C., Kovachev, L.M.: Hidden features of the soliton adaptation law to external potentials: optical and matterwave 3D nonautonomous soliton bullets. Laser Phys. **21**, 258–263 (2011)
13. Xu, S.L., Petrović, N., Belić, M.R.: Exact solutions of the $(2 + 1)$-dimensional quintic nonlinear Schrödinger equation with variable coefficients. Nonlinear Dyn. **80**, 583–589 (2015)
14. Zhong, W.P., Belić, M.R., Huang, T.W.: Two-dimensional accessible solitons in PT-symmetric potentials. Nonlinear Dyn. **70**, 2027–2034 (2012)
15. Dai, C.Q., Wang, Y.Y., Zhang, J.F.: Analytical spatiotemporal localizations for the generalized $(3 + 1)$-dimensional nonlinear Schrodinger equation. Opt. Lett. **35**, 1437–1439 (2010)
16. Baizakov, B.B., Filatrella, G., Malomed, B.A., Salerno, M.: Double parametric resonance for matter-wave solitons in a time-modulated trap. Phys. Rev. E **71**, 036619 (2005)
17. Chen, S.H., Dudley, J.M.: Spatiotemporal nonlinear optical self-similarity in three dimensions. Phys. Rev. Lett. **102**, 233903 (2009)
18. Dai, C.Q., Wang, X.G., Zhou, G.Q.: Stable light-bullet solutions in the harmonic and parity-time-symmetric potentials. Phys. Rev. A **89**, 013834 (2014)
19. Soljačić, M., Segev, M., Menyuk, C.R.: Self-similarity and fractals in soliton-supporting systems. Phys. Rev. E **61**, R1048–R1051 (2000)
20. Serkin, V.N., Hasegawa, A., Belyaeva, T.L.: Solitary waves in nonautonomous nonlinear and dispersive systems: nonautonomous solitons. J. Mod. Opt. **57**, 1456–1472 (2010)